Environmental Science & Technology

Article

pubs.acs.org/est

Effect of Ammonia on the Volatility of Organic Diacids

Andrea L. Paciga,[†] Ilona Riipinen,[‡] and Spyros N. Pandis*[,†,§]

[†]Department of Chemical Engineering, Carnegie Mellon University, Pittsburgh, Pennsylvania 15213, United States

[‡]Department of Applied Environmental Science & Bert Bolin Center for Climate Research, Stockholm University, Stockholm SE-10691, Sweden

[§]Institute of Chemical Engineering Sciences, FORTH, Patras GR-26504, Greece

ABSTRACT: The effect of ammonia on the partitioning of two dicarboxylic acids, oxalic (C2) and adipic (C6) is determined. Measurements by a tandem differential mobility analysis system and a thermodenuder (TD-TDMA) system are used to estimate the saturation vapor pressure and enthalpy of vaporization of ammonium oxalate and adipate. Ammonia dramatically lowered the vapor pressure of oxalic acid, by several orders of magnitude, with an estimated vapor pressure of $1.7 \pm 0.8 \times 10^{-6}$ Pa at 298 K. The vapor pressure of ammonium adipate was $2.5 \pm 0.8 \times 10^{-5}$ Pa at 298 K, similar to that of adipic acid. These results suggest that the dominance of oxalate in diacid concentrations measured in ambient aerosol could be attributed to the salt formation with ammonia.

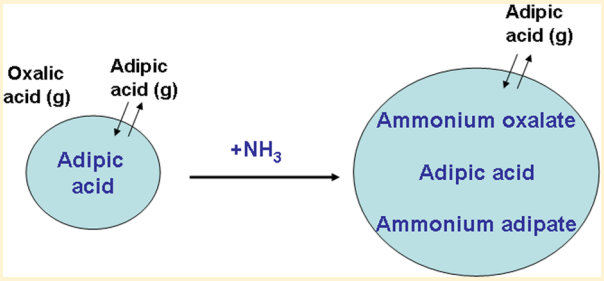

INTRODUCTION

Atmospheric aerosols have substantial influence on climate and public health.[1−4] Aerosol properties including volatility, hygroscopicity, chemical reactivity, and optical properties are directly or indirectly linked to their effects on climate.[5] However, the extent of these effects is uncertain due to the limited understanding of aerosol composition and the mechanisms for particle formation and growth. Organic matter is a major contributor to the chemical composition of fine particulate matter in the atmosphere,[6] with dry submicron particulate matter containing up to 70% organic compounds by mass.[7] Globally, attempts to characterize this fraction have covered a range of sites under various seasonal conditions; a common thread among them all is the presence of particulate dicarboxylic acids. Significant amounts of these condensed acids have been measured in urban,[8−13] remote[10,11] and marine sites,[14,15] typically with oxalic acid (C_2) being the most abundant.

A principal source of primary atmospheric diacids is vehicle emissions, where they form as products of incomplete combustion.[16] In addition to automobile exhaust, forest fires are an important source of dicarboxylic acids.[17] Organic acids have biogenic sources as well, resulting from biological processes occurring in plant roots and soil.[18] However, emissions alone cannot explain the observed concentrations of these low molecular weight acids (C_2−C_{10}).[9,19,20] Thus, several secondary production mechanisms have been proposed, including in-cloud processes,[19−22] photochemical oxidation followed by gas to particle partitioning,[23,24] and heterogeneous reactions.[10] Based on analysis of atmospheric size distributions, combinations of these theories have also been used to explain the presence of diacids in the particulate phase.[25,26]

Through similar analysis, some ambient studies[27,23] have found support for the hypothesis of stable organic salt formation with ammonia. Yang and Yu (2008)[28] reported that concentrations of oxalate in Singapore were 10−15 times greater than that of oxalic acid in aerosol particles. Evidence of organic salt formation through acid−base neutralization reactions with ammonia (or amines) has been provided by ambient data[29] and laboratory studies.[30]

Other studies, both experimental and computational, explicitly examined the role of ammonia/amines in atmospheric processing. Through a series of smog chamber experiments Angelino et al. (2001)[32] identified secondary and tertiary alkylamines as precursors to organic nitrogen-containing species found in ambient aerosol. Na et al. (2007)[33] analyzed the potential for particle formation from ammonia and α-pinene ozonolysis. Through measurements of number and volume particle size distributions, they were able to show that ammonia can react with organic acids to form condensable salts. In addition to these, several other studies[34−38] have assessed the formation of secondary organic aerosol through reactions with gas phase ammonia/amines, and suggested that these production pathways could play a significant role in aerosol chemistry.

An important thermodynamic property involved in gas to particle conversion is vapor pressure. Analysis of relative volatilities of select aminium salts proved them to be quite stable when compared to ammonium sulfate, which is a well characterized major atmospheric particulate matter compo-

Received: August 4, 2014
Revised: October 29, 2014
Accepted: October 30, 2014
Published: October 30, 2014

nent.[39] Similarly, evaluating the decrease in volatility due to the formation ammonium organic salts may provide insight into the processes responsible for particulate phase dicarboxylates. Several methods have been employed to measure the vapor pressure of these low volatility systems.[40] Some of these techniques include Knudsen effusion,[41−46] gas saturation,[47−49] and temperature-programmed thermal desorption,[49−52] all of which have been used to estimate the volatility of dicarboxylic acids. The tandem differential mobility analyzer (TDMA) technique has also been used to estimate the thermodynamic properties of dicarboxylic acids. Solid-[53−57] and liquid-[58,59] phase vapor pressures of these low volatility organic acids have been measured using this particular method. The TDMA system is typically composed of an aerosol generation source, a differential mobility analyzer (DMA) to size select particles and create a monodisperse stream, a laminar flow reactor that allows for evaporation to occur, and another DMA that measures the initial and final particle size distributions. Through the measured evaporation rate and mass transfer fundamentals, thermodynamic properties, including vapor pressure, can be quantified.

Thermodenuders (TDs) can also be incorporated in this TDMA technique to measure the volatility distribution of monodisperse aerosol systems.[60] TDs are typically composed of a heating and a cooling section. The heating section is set to a predetermined temperature allowing the aerosol to evaporate. The evaporated aerosol then enters a cooling section, usually filled with activated carbon, which removes any vapors that may recondense onto the particles. Generally a comparison between the size distribution before and after the heating is performed in order to estimate the evaporated volume. TDs have the ability to monitor evaporation over a range of volatilities, including low volatility compounds,[61] making them especially useful for field[61−65] and laboratory[60,66−68] studies.

To our knowledge, there are no estimations for the vapor pressure of ammonium-dicarboxylate salts. Ammonia has been implicated as a possible pathway for particle formation through acid−base neutralization. However, there is no quantitative data that represents the lowered volatility of dicarboxylic acids through the presence of ammonia. This work aims to estimate the vapor pressure of ammonium oxalate and ammonium adipate through TDMA-TD measurements and thermodynamic modeling. Volatility information may provide insight on the atmospheric processing of dicarboxylic acids and explain the abundance of oxalate in ambient aerosol.

EXPERIMENTAL SECTION

Materials and Methods. The experimental setup used in this study is outlined in Figure 1. The basic steps in the system involve the formation of ammonium organic salt particles, selection of particles of a specific size, exposing the almost monodisperse particles to higher temperatures in a thermodenuder (TD), and measuring the new size of the partially evaporated particles.

The ammonium salt particles are created by sending the salt solution (concentration of 1 g L^{-1} in purified water) through a constant-output atomizer (TSI model 3076). The ammonium salts tested are ammonium oxalate monohydrate (Sigma-Aldrich, > 99.5% purity) and ammonium adipate (Dr. Paul Lohmann Inc., > 98%). The particles are then sent through a diffusion dryer filled with silica gel to remove moisture. An almost monodisperse particle population is selected using a differential mobility analyzer (DMA, TSI model 3071A/3081),

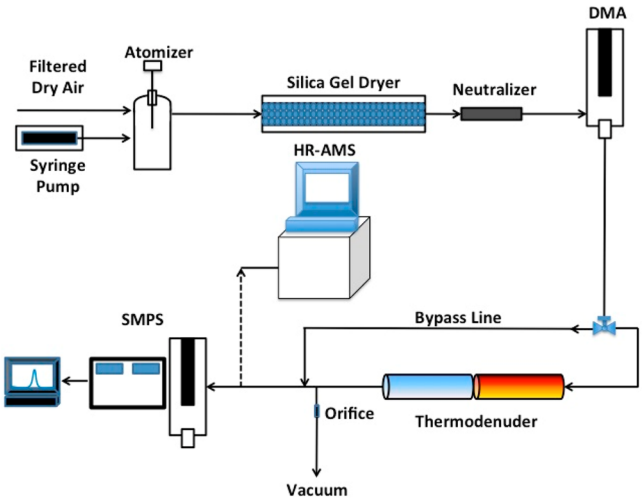

Figure 1. Schematic of experimental setup used in this study.

equipped with a 10mCi Kr-85 charger (TSI model 3077A). Particle sizes of 200, 150, and 100 nm were tested for each ammonium salt. All the experiments were conducted in RH < 10%. However, given that the particles were produced from an aqueous solution there is the potential of having some remaining water in these particles. We tested this hypothesis by adding a second drier to our system and thus giving the particles more time to equilibrate at this very low RH. We did not observe any changes.

The monodisperse particles enter the TD where they encounter elevated temperatures, promoting mass transfer of the material from the particulate to the gas phase. The TD design is detailed by Lee et al. (2010)[67] and adapted to fit the needs of this work. The thermodenuder is composed of a heating and cooling section. The heating section consists of 2 concentric stainless steel tubes with an inner tube diameter of 3.5 cm, an outer tube diameter of 6 cm, and a length of 55 cm. Heating tape is used to heat the heating section; while a thermocouple monitors the temperature. The range of TD temperature used is 25 °C through 75 °C.The cooling section is made up of a stainless steel tube with a diameter of 6.5 cm and a length of 45 cm. A tubular mesh, with a diameter of 3.5 cm, is placed in the center of the cooling section and activated carbon (Fischer Scientific, 6−14 mesh) fills the space between the mesh tube and inner diameter. In order to get a "standard" to which to compare, a bypass line (0.25 in. inner diameter) is used. The residence time in the TD and bypass was adjusted by adding a 0.61 L min^{-1} orifice (O'Keefe Controls Co.) attached to a vacuum line. This allowed for an aerosol flow rate of either 0.5 L min^{-1} or 1.11 L min^{-1}, corresponding to residence times of 32 and 14 s, respectively.

The resulting number size distributions were measured using a scanning mobility particle sizer (SMPS) following the TD. The SMPS is composed of a DMA (TSI, model 3081) and a condensation particle counter (CPC, TSI model 3010 or 3772). The results from thermodenuder experiments are presented as the fraction of aerosol volume (or mass) remaining after heating and is referred to as the Volume Fraction Remaining (VFR) or mass fraction remaining (MFR). In this study, the VFR is calculated for a monodisperse flow of ammonium salt particles under varying TD temperature and both residence times:

$$\mathrm{VFR} = \frac{(D_p)^3_{TD}}{(D_p)^3_{BY}} \quad (1)$$

where $(D_p)_{TD}$ and $(D_p)_{BY}$ are the mode diameters of the number distributions of the TD and bypass line, respectively.

The experiments were repeated several times using different batches of chemicals. The average standard deviation of the mean for the VFR was approximately 0.05. The uncertainty of the temperature measurements is ±1 °C and of the RH values ±1%.

EVAPORATION OF AMMONIUM OXALATE AND ADIPATE

Residence Time Effects and Particle Size Dependency. A major factor in estimating the evaporation kinetics in a particular system is the extent of thermodynamic equilibrium between aerosol and gas concentrations within the TD. To evaluate whether our system is in equilibrium, experiments were performed at two residence times (32 and 14 s respectively). The effect of residence time within the TD is illustrated in Figure 2. As the residence time increases, the amount of evaporated mass increases, resulting in a lower VFR for a given temperature. This suggests that the particles are not in equilibrium after 14 s, which is consistent with the predictions of Riipinen et al. (2010).[69]

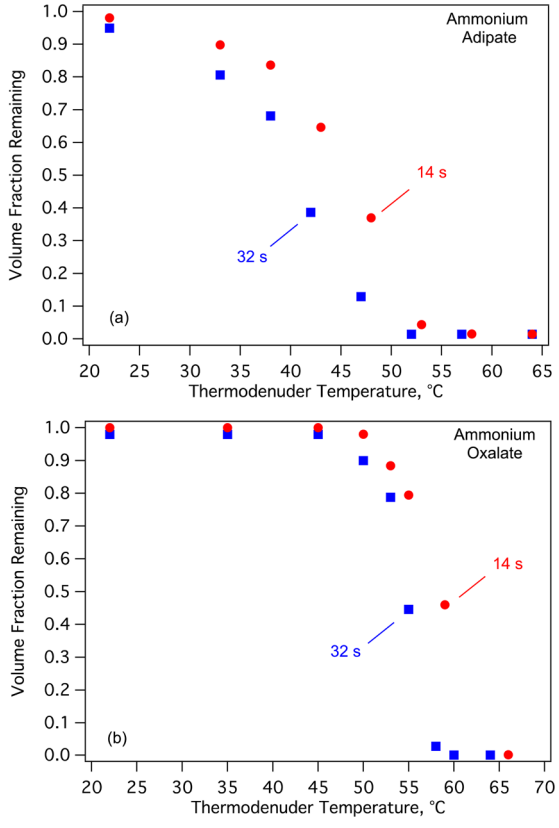

Figure 2. Measured volume fraction remaining (VFR) as a function of thermodenuder temperature for centerline residence times of 14 and 32 s for 150 nm particles of (a) ammonium adipate and (b) ammonium oxalate.

The initial particle size is another key parameter affecting VFR. Figure 3 shows the calculated VFR for various sizes of ammonium adipate and ammonium oxalate particles. Based on mass transfer principles, the VFR should decrease as particle size decreases.[60]

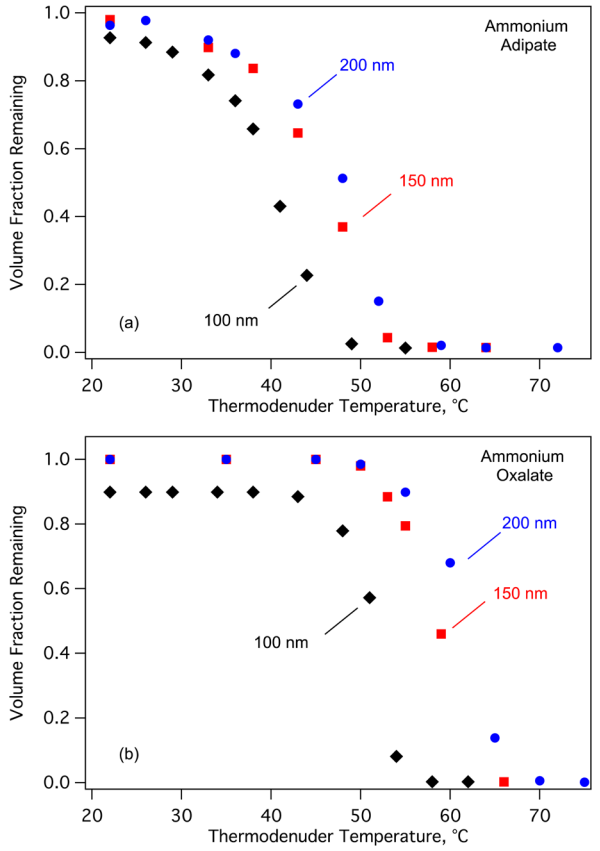

Figure 3. Measured VFR as a function of TD temperature for a centerline residence time of 14 s for 200, 150, and 100 nm particles of (a) ammonium adipate and (b) ammonium oxalate.

Estimation of Thermodynamic Properties. In order to account for the nonequilibrium state of the TD and the contributing differences in initial particle size, a dynamic mass transfer model[69] was employed to estimate the thermodynamic properties of the ammonium salts. Riipinen et al. (2010) simulated the time-dependent evaporation of multicomponent systems under varying TD conditions.

Here, a single component (ammonium oxalate, ammonium adipate) system is evaluated, simulating the residence times (32 and 14 s) and particle sizes (200, 150, 100) tested in the TDMA experimental setup. The model assumes that the particles are initially in equilibrium with the gas phase concentration before entering the TD. Other TD inputs, such as particle number concentrations and TD temperatures, were directly obtained from experimental data. Along with system conditions, compound properties must also be specified. Given the limited data on effective mass accommodation coefficients, a value of 1.0 is chosen for all simulations. In addition to the accommodation coefficient, the compound specific inputs include molecular weight, density, and diffusion coefficient. A value of 1500 kg m^{-3} was used for the density of ammonium oxalate and 1000 kg m^{-3} for ammonium adipate. The diffusion coefficients were estimated at 2×10^{-5} m^2 s^{-1} and 1.8×10^{-5} m^2 s^{-1} for ammonium oxalate and ammonium adipate respectively following the approach of Bilde et al.[54]

We explored the full parameter space for enthalpy of vaporization, saturation vapor pressure, and surface energy, using a brute-force method to account for the nonuniqueness

dx.doi.org/10.1021/es5037805 | Environ. Sci. Technol. 2014, 48, 13769−13775

of the solution. Saturation vapor pressure values of 10^{-4} to 10^{-7} Pa and enthalpy of vaporization values from 50 to 250 kJ mol^{-1} were evaluated for the ammonium adipate case. Due to the low vapor pressure of ammonium oxalate, the test range was shifted to 10^{-6} to 10^{-9} Pa for saturation vapor pressure and 100 to 300 kJ mol^{-1} for enthalpy of vaporization. For both ammonium salt cases surface tension values from 0.01 to 0.1 N m^{-2} were tested; we found that the surface energy did not influence the overall result. To determine the "best" fit, the discrepancy between modeled and experimental MFR points was calculated for all experiments and the parameter values (enthalpy of vaporization and vapor pressure) corresponding to the minimum average error were selected. Figure 4 shows the

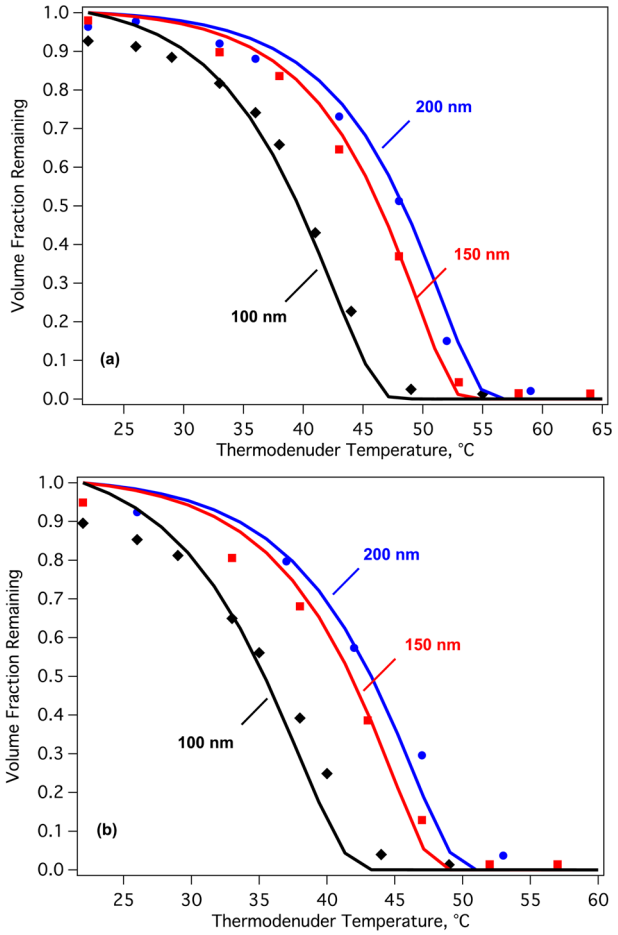

Figure 4. Measured (markers) and modeled (solid trace) VFR as a function of TD temperature for ammonium adipate particles at a centerline residence time of (a) 14 and (b) 32 s.

agreement between model results and experimental data presented for ammonium adipate particles with a vapor pressure of 2.5×10^{-5} Pa, enthalpy of vaporization of 141 kJ mol^{-1}. Figure 5 shows the model fit for ammonium oxalate particles for the parameters corresponding to the minimum error: a saturation vapor pressure of 1.7×10^{-6} Pa, enthalpy of vaporization of 192 kJ mol^{-1}. There is a small unexpected evaporation of the 100 nm particles to approximately 97 and 94 nm after 14 and 32 s in the thermodenuder, respectively. While this behavior could be explained by the existence of a more volatile compound in the particles (including water, oxalic acid, etc.) our efforts to remove it before the particles entered the thermodenuder (adding a second drier and an activated carbon

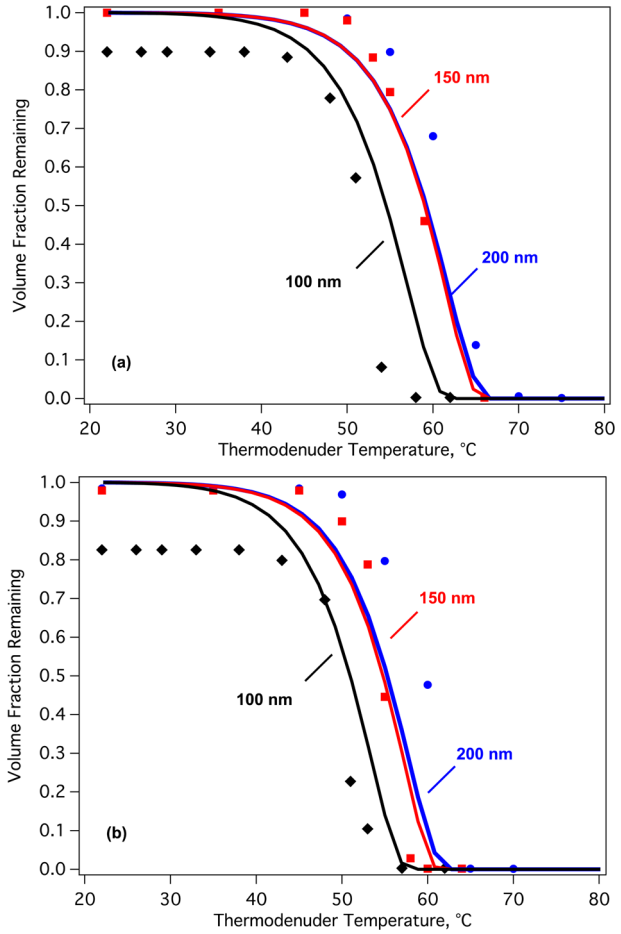

Figure 5. Measured (markers) and modeled (solid trace) VFR as a function of TD temperature for ammonium oxalate particles at a centerline residence time of (a) 14 and (b) 32 s.

denuder) were unsuccessful. This evaporation did not influence our fits and thus final results.

The saturation vapor pressure for ammonium oxalate is 4 orders of magnitude lower than that of oxalic acid (Table 1). This substantial decrease is due to the strong salt formation with ammonia. However, the vapor pressure and enthalpy of vaporization does not vary significantly between ammonium

Table 1. Estimated Thermodynamic Properties

compound	vapor pressure at 298 K (Pa)	enthalpy of vaporization at 298 K (kJ mol^{-1})	source
oxalic acid	$2.2 \pm 1.2 \times 10^{-2}$	75 ± 19	Booth et al. (2009)[45]
ammonium oxalate	$1.7 \pm 0.8 \times 10^{-6}$	192 ± 13	this study[a]
adipic acid	$6.1 \pm 3.9 \times 10^{-6}$	125 ± 40	Booth et al. (2009)[45]
	$3.3 \pm 0.9 \times 10^{-5}$	132 ± 8	Saleh et al. (2010)[56]
	3.0×10^{-5}	146	Chattopadhyay et al. (2005)[50]
ammonium adipate	$2.5 \pm 0.8 \times 10^{-5}$	141 ± 13	this study

[a]The values in this study are presented as the mean $\pm 2\ \sigma_{mean}$. These values have been estimated assuming an accommodation coefficient equal to unity.

dx.doi.org/10.1021/es5037805 | Environ. Sci. Technol. 2014, 48, 13769−13775

adipate and adipic acid. Based on ambient data and the chemical properties of the diacids, these results could explain (together with the high water solubility) the high concentrations of oxalate in particulate phase.

Relative Volatility Comparison. Oxalic acid exists mainly as oxalate in the particulate phase,[28] supporting the idea that salt formation could be a pathway for forming particulate phase oxalate. The acid dissociation constant, K_a, is an indicator of the strength of an acid, and thereby how strong of a salt it will form. Generally, values are presented as the negative logarithm of the acid dissociation constant, pK_a. A comparison of these pK_a values (Table 2) shows that oxalic acid is a stronger acid than adipic acid. This may provide some insight on the relative strengths of their ammonium salts. For a given initial particle size and TD residence time, the volatility of ammonium oxalate and ammonium adipate were analyzed. Although ammonium adipate is a larger molecule (having a molecular weight of 180 g mol^{-1} compared to ammonium oxalate's 124 g mol^{-1}), it is more volatile than ammonium oxalate (Figures 6 and 7). This result is consistent with the acid dissociation constants of oxalic and adipic acid. These findings are also consistent with the observations of Ortiz-Montalvo et al.[70] who observed significant reduction of the volatility and increase of the enthalpy of vaporization of the SOA produced from glyoxal and explained it, at least to large extent, with the conversion of the oxalate to ammonium oxalate. The significant reduction of volatility due to the reaction with ammonia appears to be a specific property of oxalic acid and may not be applicable to most of the other atmospheric diacids.

Table 2. pK_a Values for Oxalic and Adipic Acid[71]

compound	pK_{a1}	pK_{a2}
oxalic acid	1.23	4.19
adipic acid	4.43	5.41

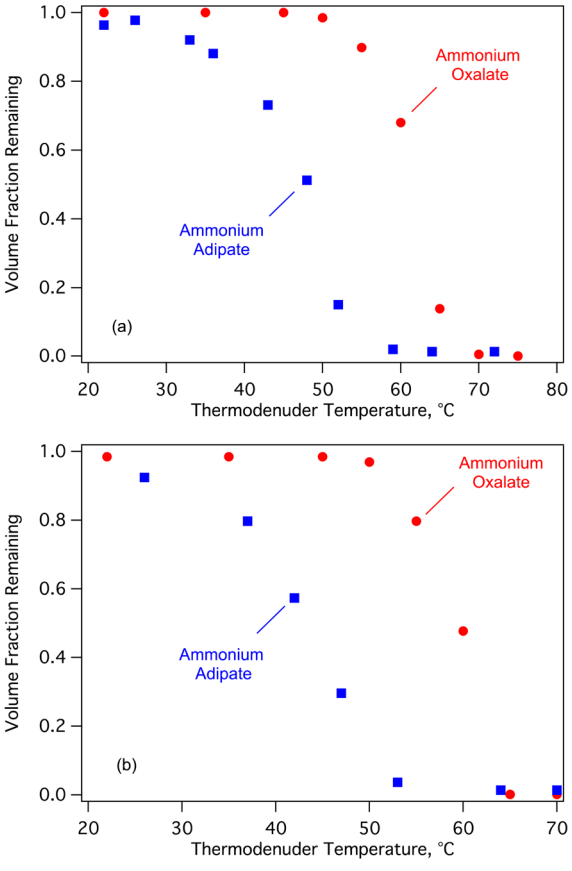

Figure 6. Relative volatility comparison showing measured VFR as a function of TD temperature for 200 nm particles of ammonium adipate and ammonium oxalate at a centerline residence time of (a) 14 s and (b) 32 s.

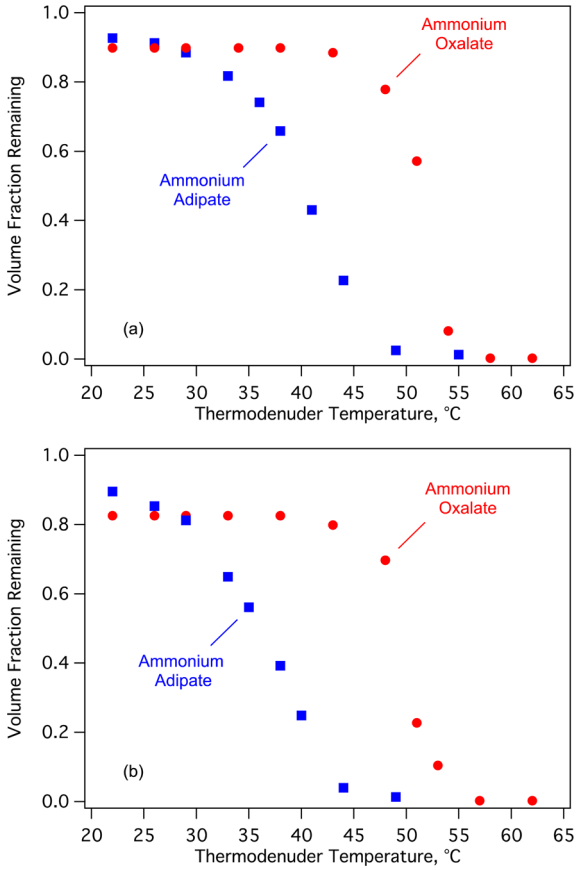

Figure 7. Relative volatility comparison showing measured VFR as a function of TD temperature for 100 nm particles of ammonium adipate and ammonium oxalate at a centerline residence time of (a) 14 s and (b) 32 s.

AUTHOR INFORMATION

Corresponding Author

*Phone: 1-412-268-3531; fax: 1-412-268-7139; e-mail: spyros@andrew.cmu.edu.

Notes

The authors declare no competing financial interest.

ACKNOWLEDGMENTS

This project was supported by the EPA STAR program and the EU FP7-IDEAS-ERC ATMOPACS project.

REFERENCES

(1) Dockery, D. W.; Pope, C. A., III Accute respiratory effects of particulate air pollution. *Ann. Rev. of Public Health* **1994**, *15*, 107−132.
(2) Nel, A. Air pollution-related illness: Effects of particles. *Science* **2005**, *308*, 804−806.
(3) Pope, C. A., III; Ezzati, M.; Dockery, D. W. Fine particulate air pollution and life expectancy in the United States. *New Eng. J. Med.* **2009**, *360*, 376−386.

(4) Intergovernmental Panel on Climate Change (IPCC). *Climate Change 2001: The Physical Science Basis*, 2007.
(5) Poschl, U. Atmospheric aerosols: Composition, transformation, climate, and health effects. *Angew. Chem. Int. Ed.* **2005**, *44*, 7520−7540.
(6) Kanakidou, M.; Seinfeld, J. H.; Pandis, S. N.; Barnes, I.; Dentener, F. J.; Facchini, M. C.; Van Dingenen, R.; Ervens, B.; Nenes, A.; Nielsen, C. J.; Swietlicki, E.; Putaud, J. P.; Balkanski, Y.; Fuzzi, S.; Horth, J.; Moortgat, G. K.; Winterhalter, R.; Myhre, C. E. L.; Tsigaridis, K.; Vignati, El.; Stpanou, E. G.; Wilson, J. Organic aerosol and global climate modelling: A review. *Atmos. Chem. Phys.* **2005**, *5*, 1053−1123.
(7) Zhang, Q.; Jimenez, J. L.; Canagaratna, M. R.; Allan, J. D.; Coe, H.; Ulbrich, I.; Alfarra, M. R.; Takami, A.; Middlebrook, A. M.; Sun, Y. L.; Dzepina, K.; Dunlea, E.; Docherty, K.; DeCarlo, P. F.; Salcedo, D.; Onasch, T.; Jayne, J. T.; Miyoshi, T.; Shimono, A.; Hatakeyama, S.; Takegawa, N.; Kondo, Y.; Scheider, J.; Drewnick, F.; Borrman, S.; Weimer, S.; Demerjian, K.; Williams, P.; Bower, K.; Bahreini, R.; Cottrell, L.; Griffin, R. J.; Rautianinen, J.; Sun, J. Y.; Zhang, Y. M.; Worsnop, D. R. Ubiquity and dominance of oxygenated species in organic aerosols in athropogenically-influenced Northern Hemisphere midlatitudes. *Geophys. Res. Lett.* **2007**, *34*, L13801 DOI: 10.1029/2007 GL029979.
(8) Sempere, R.; Kawamura, K. Comparative distributions of carboxylic acids and related polar compounds in snow, rain and aerosols from urban atmosphere. *Atmos. Environ.* **1994**, *28*, 449−459.
(9) Limbeck, A.; Puxbaum, H. Organic acids in continental background aerosols. *Atmos. Environ.* **1999**, *33*, 1847−1852.
(10) Kerminen, V.-M.; Ojanen, C.; Pakkanen, T.; Hillamo, R.; Aurela, M.; Merilainen, J. Low molecular weight dicarboxylic acids in an urban and rural atmosphere. *J. Aerosol Sci.* **2000**, *31*, 349−362.
(11) Rohrl, A.; Lammel, G. Low molecular weight dicarboxylic acids and glyoxylic acid: Seasonal and air mass characteristics. *Environ. Sci. Technol.* **2001**, *35*, 95−101.
(12) Wang, G.; Niu, S.; Liu, C.; Wang, L. Identification of dicarboxylic acids and aldehydes of PM_{10} and $PM_{2.5}$ aerosols in Nanjinh, China. *Atmos. Environ.* **2002**, *36*, 1941−1950.
(13) Yao, X.; Fang, M.; Chan, C. K.; Ho, K. F.; Lee, S. C. Characterization of dicarboxylic acids in $PM_{2.5}$ in Hong Kong. *Atmos. Environ.* **2004**, *28*, 963−970.
(14) Mochida, M.; Kawamura, K.; Umemoto, N.; Kobayashi, M.; Matsunaga, S.; Lim, H.-J.; Tuprin, B. J.; Bates, T. S.; Simoneit B. R. T. Spatial distributions of oxygenated organic compounds (dicarboxylic acids, fatty acids, and levoglucosan) in marine aerosols over the western Pacific and off the coast of East Asia: Contintental outflow of organic aerosols during the ACE-Asia campaign. *J. Geophys. Res.* **2003**, *108*, DOI: 10.1029/2002 JD003249.
(15) Wang, H.; Kawamura, K.; Yamazaki, K. Water-soluble dicarboxylic acids, ketoacids and dicarbonyls in the atmospheric aerosols over the Southern Ocean and Western Pacific Ocean. *J. Atmos. Chem.* **2006**, *53*, 43−61.
(16) Kawamura, K.; Kaplan, I. R. Motor exhaust emissions as a primary source for dicarboxylic acids in Los Angeles ambient air. *Environ. Sci. Technol.* **1987**, *21*, 105−110.
(17) Narukawa, M.; Kawamura, K. Distribution of dicarboxylic acids and carbon isotopic compositions in aerosols from 1997 Indonesian forest fires. *Geophys. Res. Lett.* **1999**, *26*, 3101−3104.
(18) Jones, D. L. Organic acids in the rhisosphere. *Plant Soil.* **1998**, *205*, 25−44.
(19) Sorooshian, A.; Vautbangkul, V.; Brechtel, F. J.; Ervens, B.; Feingold, G.; Bahreini, R.; Murphy, S. M.; Holloway, J. S.; Atlas, E. L.; Buzorius, G.; Jonsson, H.; Flagan, R. C.; Seinfeld, J. H. Oxalic acid in clear and cloudy atmospheres: Analysis of data from International Consortium for Atmospheric Research on Transport and Transformation 2004. *J. Geophys. Res.* **2006**, *111*, DOI: 10.1029/2005JD006880.
(20) Yu, J. Z.; Huang, X.-F.; Xu, J.; Hu, M. When aerosol sulfate goes up, so does oxalate: Implication for the formation mechanisms of oxalate. *Environ. Sci. Technol.* **2005**, *39*, 128−133.
(21) Yao, X.; Fang, M.; Chan, C. K. Size distributions and formation of dicarboxylic acids in atmospheric particles. *Atmos. Environ.* **2002**, *36*, 2099−2107.
(22) Blando, J. D.; Turpin, B. J. Secondary organic aerosol formation in cloud and fog droplets: A literature evaluation of plausibility. *Atmos. Environ.* **2000**, *34*, 1623−1632.
(23) Martinelango, P. K.; Dasgupta, P. K.; Al-Horr, R. S. Atmospheric production of oxalic/acid oxalate and nitric acid/nitrate in the Tampa Bay airshed: Parallel pathways. *Atmos. Environ.* **2007**, *41*, 4258−4269.
(24) Kawamura, K.; Kasukabe, H.; Barrie, L. A. Source and reaction pathways of dicarboxylic acids, ketoacids, and dicarbonyls in arctic aerosols: One year of observations. *Atmos. Environ.* **1996**, *30*, 1709−1722.
(25) Yang, F.; Chen, H.; Wang, X.; Yang, X.; Du, J.; Chen, J. Single particle mass spectrometry of oxalic acid in ambient aerosols in Shanghai: Mixing state and formation mechanism. *Atmos. Environ.* **2009**, *43*, 3876−3882.
(26) Yao, X.; Lau, A. P. S.; Fang, M.; Chan, C. K.; Hu, M. Size distributions and formation of ionic species in atmospheric particulate pollutants in Beijing, China: 2-dicarboxylic acids. *Atmos. Environ.* **2003**, *37*, 3001−3007.
(27) Lefer, B. L.; Talbot, R. W. Summertime measurements of aerosol nitrate and ammonium at a northeastern US site. *J. Geophys. Res.* **2001**, *106*, 20365−20378.
(28) Yang, L.; Yu, L. E. Measurements of oxalic acid, oxalates, malonic acid, and malonates in atmospheric particulates. *Environ. Sci. Technol.* **2008**, *42*, 9268−9275.
(29) Wang, X.; Gao, S.; Yang, X.; Chen, H.; Chen, J.; Zhuang, G.; Surratt, J. D.; Chan, M. N.; Seinfeld, J. H. Evidence of high molecular weight nitrogen-containing organic salts in urban aerosols. *Environ. Sci. Technol.* **2010**, *44*, 4441−4446.
(30) Dinar, E.; Anttila, T.; Rudich, Y. CCN activity and hygroscopic growth of organic aerosols following reactive uptake of ammonia. *Environ. Sci. Technol.* **2008**, *42*, 793−799.
(31) Mensah, A. A.; Buchholz, A.; Mentel, Th.F.; Tillmann, R.; Kiendler-Scharr, A. Aerosol mass spectrometric measurements of stable crystal hydrates of oxalates and inferred relative ionization efficiency of water. *J. Aerosol. Sci.* **2011**, *42*, 11−19.
(32) Angelino, S.; Suess, D. T.; Prather, K. A. Formation of aerosol particles from reactions of secondary and tertiary alkylamines: Characterization by Aerosol Time-of-Flight Mass Spectrometry. *Environ. Sci. Technol.* **2001**, *35*, 3130−3138.
(33) Na, K.; Song, C.; Switzer, C.; Cocker, D. R., III. Effect of ammonia on secondary organic aerosol formation from a-pinene ozonolysis in dry and humid conditions. *Environ. Sci. Technol.* **2007**, *41*, 6096−6102.
(34) Murphy, S. M.; Sorooshian, A.; Kroll, J. H.; Ng, N. L.; Chhabra, P.; Tong, C.; Surratt, J. D.; Knipping, E.; Flagan, R. C.; Seinfeld, J. H. Secondary aerosol formation from atmospheric reactions of aliphatic amines. *Atmos. Chem. Phys.* **2007**, *7*, 2313−2337.
(35) Silva, P. J.; Erupe, M. E.; Price, D.; Elias, J. Trimethylamine as precursor to secondary organic aerosol formation via nitrate radical reaction in the atmosphere. *Environ. Sci. Technol.* **2008**, *42*, 4689−4696.
(36) Kurten, T.; Loukonen, V.; Vehkamaki, H.; Kulmala, M. Amines are likely to enhance neutral and ion-induced sulfuric acid-water nucleation in the atmosphere more effectively than ammonia. *Atmos. Chem. Phys.* **2008**, *8*, 4095−4103.
(37) Barsanti, K. C.; McMurry, P. H.; Smith, J. N. The potential contribution of organic salts to new particle growth. *Atmos. Chem. Phys.* **2009**, *9*, 2949−2957.
(38) Malloy, Q. G. J.; Qi, L.; Warren, B.; Crocker, D. R., III.; Erupe, M. E.; Silva, P. J. Secondary organic aerosol formation from primary aliphatic amines with NO_3 radical. *Atmos. Chem. Phys.* **2009**, *9*, 2051−2060.
(39) Smith, J. N.; Barsanti, K. C.; Friedli, H. R.; Ehn, M.; Kulmala, M.; Collins, D. R.; Scheckman, J. H.; Williams, B. J.; McMurry, P. H. Observations of aminium salts in atmospheric Nanoparticles and possible climatic implications. *PNAS.* **2010**, *107*, 6634−6639.

(40) Delle Site, A. The vapor pressure of environmentally significant organic chemicals: A review of methods and data at ambient temperature. *J. Phys. Chem. Ref. Data* **1997**, *26*, 157−193.
(41) Hallquist, M.; Wangberg, I.; Ljungstrom, E. Atmospheric fate of carbonyl oxidation products originating from α-pinene and Δ^3-carene: Determination of rate of reaction with OH and NO_3 radicals, UV absorption cross sections, and vapor pressures. *Environ. Sci. Technol.* **1997**, *31*, 3166−3172.
(42) Bradley, R. S.; Cotson, S. J. The vapour pressure and lattice energy of hydrogen-bonded crystals: Part II. α- and β-anhydrous oxalic acid and tetragonal pentaerythritol. *J. Chem. Soc.* **1953**, 1684−1688.
(43) Davies, M.; Thomas, G. H. The lattice energies, infra-red spectra, and possible cyclization of some dicarboxylic acids. *Trans. Faraday Soc.* **1960**, *56*, 185−192.
(44) Riberio da Silva, M. A. V.; Monte, M. J. S.; Riberio, J. R. Vapour pressures and the enthalpies and entropies of sublimation of five dicarboxylic acids. *J. Chem. Thermo.* **1999**, *31*, 1093−1107.
(45) Booth, A. M.; Markus, T.; McFiggans, G.; Percival, C. J.; Mcgillen, M. R.; Topping, D. O. Design and construction of a simple Knudsen Effusion Mass Spectrometer (KEMS) system for vapour pressure measurements of low volatility organics. *Atmos. Meas. Technol.* **2009**, *2*, 355−361.
(46) Booth, A. M.; Barley, M. H.; Topping, D. O.; McFiggans, G.; Garforth, A.; Percival, C. J. Solid state and sub-cooled liquid vapour pressures of substituted dicarboxylic acids using Knudsen Effusion Mass Spectrometry (KEMS) and Differential Scanning Calorimetry. *Atmos. Chem. Phys.* **2010**, *10*, 4879−4892.
(47) Carruth, G. F.; Kobayashi, R. Vapor pressure of normal paraffins ethane through n-decane from their triple points to about 10 mm mercury. *J. Chem. Eng. Data* **1973**, *18*, 115−126.
(48) Widegren, J. A.; Bruno, T. J. Vapor Pressure Measurements on Low-Volatility Terpenoid Compounds by the Concatenated Gas Saturation Method. *Environ. Sci. Technol.* **2010**, *44*, 388−393.
(49) Chattopadhyay, S.; Tobias, H. J.; Ziemann, P. J. A method for measuring vapor pressures of low-volatility organic aerosol compounds using a thermal desorption particle beam mass spectrometer. *Anal. Chem.* **2001**, *73*, 3797−3803.
(50) Chattopadhyay, S.; Ziemann, P. J. Vapor pressures of substituted and unsubstituted monocarboxylic and dicarboxylic acids measured using an improved thermal desorption particle beam mass spectrometry method. *Aerosol Sci. Technol.* **2005**, *39*, 1085−1100.
(51) Cappa, C. D.; Lovejoy, E. R.; Ravishankara, A. R. Determination of evaporation rates and vapor pressures of very low volatility compounds: A study of the C_4-C_{10} and C_{12} dicarboxylic acids. *J. Phys. Chem.A* **2007**, *111*, 3099−3109.
(52) Cappa, C. D.; Lovejoy, E. R.; Ravishankara, A. R. Evaporation rates and vapor pressures of the even numbered C_8-C_{18} monocarboxylic acids. *J. Phys. Chem.A* **2008**, *112*, 3959−3964.
(53) Tao, Y.; McMurry, P. H. Vapor pressures and surface free energies of C_{14}-C_{18} monocarboxylic acids and C_5 and C_6 dicarboxylic acids. *Environ. Sci. Technol.* **1989**, *23*, 1519−1523.
(54) Bilde, M.; Svenningsson, B.; Monster, J.; Rosenorn, T. Even-odd alternation of evaporation rates and vapor pressures of C_3-C_9 dicarboxylic acid aerosols. *Environ. Sci. Technol.* **2003**, *37*, 1371−1378.
(55) Monster, J.; Rosenorn, T.; Svenningsson, B.; Bilde, M. Evaporation of methyl- and dimethyl-substituted malonic, succinic, glutaric and adipic acid particles at ambient temperatures. *J. Aerosol. Sci.* **2004**, *35*, 1453−1465.
(56) Saleh, R.; Khlystov, A.; Shihadeh, A. Effect of aerosol generation method on measured saturation pressure and enthalpy of vaporization for dicarboxylic acid aerosols. *Aerosol Sci. Technol.* **2010**, *44*, 302−307.
(57) Salo, K.; Jonsson, A. M.; Andersson, P. U.; Hallquist, M. Aerosol volatility and enthalpy of sublimation of carboxylic acids. *J. Phys. Chem.A* **2010**, *114*, 4586−4594.
(58) Koponen, I. K.; Riipinen, I.; Hienola, A.; Kulmala, M.; Bilde, M. Thermodynamic properties of malonic, succinic, and glutaric acids: Evaporation rates and saturation vapor pressures. *Environ. Sci. Technol.* **2007**, *41*, 3926−3933.
(59) Riipinen, I.; Koponen, I. K.; Frank, G. P.; Hyvarinen, A.-P.; Vanhanen, J.; Lihavainen, H.; Lehtinen, K. E. J.; Bilde, M.; Kulmala, M. Adipic and malonic acid aqueous solutions: Surface tensions and saturation vapor pressures. *J. Phys. Chem.* **2007**, *111*, 12995−13002.
(60) An, W. J.; Pathak, R. K.; Lee, B.-H.; Pandis, S. N. Aerosol volatility measurement using an improved thermodenuder: Application to secondary organic aerosol. *J. Aerosol. Sci.* **2007**, *38*, 305−314.
(61) Pratt, K. A.; Prather, K. A. Real time, single particle volatility, size, and chemical composition measurements of aged urban aerosols. *Environ. Sci. Technol.* **2009**, *43*, 8276−8282.
(62) Wehner, B.; Philippin, S.; Wiedensohler, A.; Scheer, V.; Vogt, R. Variability of non-volatile fractions of atmospheric aerosol particles with traffic influence. *Atmos. Environ.* **2004**, *34*, 6081−6090.
(63) Dzepina, K.; Volkamer, R. M.; Madronich, S.; Tulet, P.; Ulbrich, I. M.; Zhang, Q.; Cappa, C. D.; Ziemann, P. J.; Jimenez, J. L. Evaluation of recently proposed secondary organic aerosol models for a case study in Mexico City. *Atmos. Chem. Phys.* **2009**, *9*, 5681−5709.
(64) Huffman, J. A.; Docherty, K. S.; Aiken, A. C.; Cubison, M. J.; Ulbrich, I. M.; DeCarlo, P. F.; Sueper, D.; Jayne, J. T.; Worsnop, D. R.; Ziemann, P. J.; Jimenez, J. L. Chemically-resolved aerosol volatility measurements from two megacity field studies. *Atmos. Chem. Phys.* **2009**, *9*, 7161−7182.
(65) Lee, B. H.; Kostenidou, E.; Hildebrandt, L.; Riipinen, I.; Engelhart, G. J.; Mohr, C.; DeCarlo, P. F.; Mihalopoulos, N.; Prevot, A. S. H.; Baltensperger, U.; Pandis, S. N. Measurement of the ambient organic aerosol volatility distribution: Application during the Finokalia Aerosol Measurement Experiment (FAME-2008). *Atmos. Chem. Phys.* **2010**, *10*, 12149−12160.
(66) Saleh, R.; Walker, J.; Khlystov, A. Determination of saturation pressure and enthalpy of vaporization of semi-volatile aerosols: The integrated volume method. *J. Aerosol Sci.* **2008**, *39*, 876−887.
(67) Faulhaber, A. E.; Thomas, B. M.; Jimenez, J. L.; Jayne, J. T.; Worsnop, D. R.; Ziemann, P. J. Characterization of a thermodenuder-particle beam mass spectrometer system for the study of organic aerosol volatility and composition. *Atmos. Meas. Technol.* **2009**, *2*, 15−31.
(68) Grieshop, A. P.; Miracolo, M. A.; Donahue, N. M.; Robinson, A. L. Constraining the volatility distribution and gas-particle partitioning of combustion aerosols using isothermal dilution and thermodenuder measurements. *Environ. Sci. Technol.* **2009**, *43*, 4750−4756.
(69) Riipinen, I.; Pierce, J. R.; Donahue, N. M.; Pandis, S. N. Equilibration time scales of organic aerosol inside thermodenuders: Evaporation kinetics versus thermodynamics. *Atmos. Environ.* **2010**, *44*, 597−607.
(70) Ortiz-Montalvo, D. L.; Hakkinen, S. A. K.; Schwier, A. N.; Lim, Y. B.; McNeil, V. F.; Turpin, B. J. Ammonium addition (and aerosol pH) has a dramatic impact on the volatility and yield of glyoxal secondary organic aeosol. *Environ. Sci. Technol.* **2014**, *48*, 255−262.
(71) Serjeant, E. P.; Dempsey, B. *Ionization Constants of Organic Acids in Aqueous Solution*; Pergamon, Oxford, 1979.